The International Journal of Advanced Manufacturing Technology (2024) 134:445–451
https://doi.org/10.1007/s00170-024-14152-z

ORIGINAL ARTICLE

Microstructure, microhardness, and tribological behavior of Ti-6Al-4 V nitrided by laser irradiation

Hamza Essoussi[1] · **Fatima Zahra Bougueraa**[1] · **Said Ettaqi**[1]

Received: 21 March 2024 / Accepted: 15 July 2024 / Published online: 22 July 2024

Abstract

The aim of this article is to determine the microhardness, the tribological behavior, and the microstructure of a Ti-6Al-4 V alloy nitrided with a pulsed Nd-YAG (neodymium-doped yttrium aluminum garnet) laser under nitrogen gas flow. The Ti alloy's surface was irradiated and melted at different laser scanning speeds. X-ray diffraction revealed three phases: α-Ti, TiN, and $TiN_{0.3}$. Optical and scanning electron microscopy results revealed dendritic microstructure in both laser-melted and nitrided zones with TiN dendrites concentrated near the alloy's surface. Furthermore, surface's wear examination using pin-on-disk tribometer revealed that the wear morphology depends on the thickness of the TiN nitrided layer (2–8 µm); thus, the enhanced wear resistance is observed in the case of the sample with thicker TiN layer obtained under a laser beam speed of 2.5 mm/s.

Keywords Ti-6Al-4 V nitridation · Laser melting · Microstructure · Microhardness · Friction coefficient

1 Introduction

Pure titanium and titanium alloys exhibit excellent properties such as strong corrosion resistance and high strength-to-weight ratio. Their lightness and ability to resist to extreme temperatures make these materials suitable for aeronautics and space industry [1–6]. Moreover, due to its exceptional biocompatibility, close to that of other biomaterials, it is mostly attributable to the perfect balance of strong corrosion resistance and suitable reactivity [7–9]. Titanium and majority of its alloys have gained recently a growing interest in medical domain. However, their disadvantages are the strong friction and the poor wear resistance; to overcome these disadvantages, laser-based method is a kind of surface hardening methods widely applied to improve the surface performance of titanium alloys by giving rise to the formation of ceramic particles such as titanium carbide (TiC) [10], titanium boride (TiBr) [11], silicon carbide (SiC) [12], and titanium nitride (TiN) [13].

In conventional nitriding treatments, such as gas nitriding and plasma nitriding [13], the entire substrate material is mainly affected by the process parameters acting on the whole subtract leading to performance degradation and unwanted substrate deformation, while the nitridation of pure titanium and its alloys using laser to generate locally ultra-fast heating and cooling has been widely studied with the objective to generate hardened and micrometer-thick nitride layer within seconds, resulting in better tribological response [13, 14].

The applicability of this laser-based technology to modify the surface of titanium alloys has been proved. Zeng and workers [15], who investigated titanium nitridation produced on commercially pure titanium samples using the laser surface nitriding technique, discovered that using different laser scanning speeds and regulated N_2 atmosphere, distinct titanium nitride coatings with varying thicknesses, phase components, composition, and roughness were created. Moreover, laser power, beam size, scanning speed, and nitrogen concentration in the environment are among the main laser nitriding parameters playing a major role on affecting the complex

Highlights.
- Solid-state laser nitridation creates a nitride layer on Ti6Al-4V alloy surface.
- The nitrided layer is made up of α-Ti, TiN, and $TiN_{0.3}$ phases.
- Laser nitrided samples show an increased hardness and wear resistance to roughly five times that of substrates.

✉ Hamza Essoussi
hamza.essoussi1@gmail.com

[1] Laboratory of Energy, Materials and Sustainable Development, ENSAM, Moulay Ismail University, 15290 Meknes, Morocco

microstructures obtained after the solidification of the laser-melted zone (LMZ). On the other hand, Senthilselvan [16] worked on high-power diode laser nitriding of titanium in nitrogen gas and succeeded in producing a unique golden-colored TiN surface with superior wear resistance and a hardness six times that of the substrate. The microstructures of this laser nitrided titanium were dendrite and martensite. To accomplish nitridation without surface melting on Ti-6Al-4 V substrates, Man [17] has used a 3-mm laser spot diameter, a nitrogen flow rate of 40 l/min, an ideal laser power, and a scanning speed of 250 W and 1 mm/s, respectively. Their results revealed that the hardness increased by nearly 2.3 times than that of the substrate, while the wear resistance rose by approximately eight times.

In this study, nitridation was conducted using pulsed Nd-YAG laser and a nitrogen atmosphere under four scanning speeds on Ti-6Al-4 V titanium alloy aiming to enhance its hardness and its wear resistance. A lot of attention is given to the surface performance and the microstructural characteristics of the nitrided samples.

2 Experimental procedures

Substrates used in this study were square foils (18×18 mm^2) of Ti-6Al-4 V titanium alloy, 3 mm thick. Their chemical composition is presented in Table 1.

The used laser irradiation device was a pulsed Nd-YAG source, the wavelength of laser radiation was 1.064 μm, whereas the maximum transmitted power was 300W. The beam diameter on the sample surface was about 0.5 mm. The used irradiation conditions are given in Table 2.

Substrate surface was polished to give a uniform surface state and cleaned just before the laser irradiation. The surface hardening of Ti-6Al-4 V was performed by nitridation under gaseous nitrogen flow during laser melting. The substrates were moved under the stationary laser beam using a numerically controlled table. The laser irradiation parameters used in this study were 3 J pulse energy, 3 ms pulse time, 50 Hz pulse frequency, and beam scanning speeds in the range from 2.5 to 10 mm/s.

To identify the crystallized phases present in the nitrided LMZ, X-ray diffraction using Cu-K_α radiation was performed, while for microstructural examination of the nitrided surfaces, optical and scanning electron microscopes were used after mounting, polishing the cross-section of the nitrided surfaces and etching using Kroll's reagent.

The friction tests were carried out in air and at room temperature using a pin-on-disk tribometer; the friction action was provided by a 6-mm-diameter ruby ball under a constant normal load of 5 N and a rotating at velocity of 200 rpm over a non-lubricated surface. The duration of friction test corresponds to 8000 turns. Vickers microhardness was measured on the sample's cross-section under a load of 200 gf and dwell time of 10 s.

Table 2 Processing conditions used to nitride Ti-6Al-4 V titanium alloy

Samples	a	b	c	d
Beam scanning speeds (mm/s)	10	7.5	5	2.5
Pulse energy (J)	3			
Pulse time (ms)	3			
Pulse frequency (Hz)	50			
Nitrogen flow rate (l/min)	10			

3 Results and discussion

3.1 Phase analysis and microstructure

The phases generated by solidification after melting under laser irradiation and reaction between nitrogen and Ti-6A1-4 V titanium alloy were identified by X-ray diffraction. For all samples, the X-ray diffraction pattern was similar to that shown in Fig. 1, which indicated the presence in the laser-melted zone (LMZ) of alpha-titanium (α-Ti) and two ceramic phases: the first corresponds to cubic titanium nitride (TiN) and the second matches with the hexagonal titanium nitride ($TiN_{0.3}$). Alpha-titanium and cubic titanium nitride were the prevalent phases.

The optical surface morphology of laser-nitrided Ti-6A1-4 V alloy for scanning speed of 2.5 mm/s shown in Fig. 2 revealed the presence of a periodic relief resulting from the melting and solidification phenomena generated by the multipass pulsed irradiation; it can be seen also the presence of periodic golden color due to the formation of TiN phase. Moreover, with the increasing of scanning speed, the golden color becomes irregular along the width direction.

From the SEM micrograph shown Fig. 3, it represents the cross-section of the typical micrograph of the nitrided samples. Three distinct zones can be easily distinguished. First, the so-called laser-melted zone (LMZ) with an average thickness of about 8 µm, containing a great quantity of titanium nitrides which include TiN dendrites and a needle-shaped phase enclosed in the Ti matrix is observed in the top area. The TiN dendrites were concentrated in the top

Table 1 Chemical composition of the substrate

Alloying elements	Al	V	C	Fe	O	Ti
Wt.%	6.13	3.92	142 ppm	1552 ppm	1064 ppm	Bal

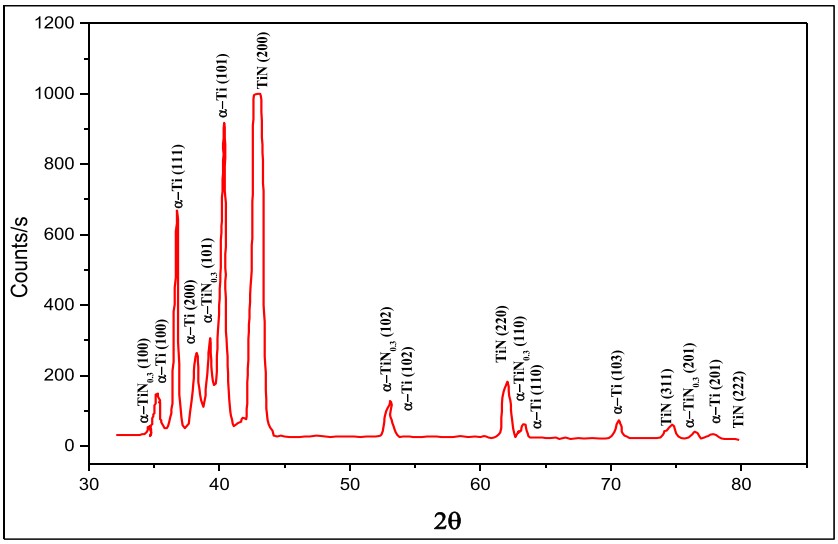

Fig. 1 Typical X-ray diffraction pattern exhibited by a surface of Ti-6Al-4 V titanium alloy nitrided under nitrogen flow l0 l/min and beam scanning speed of 2.5 mm/s

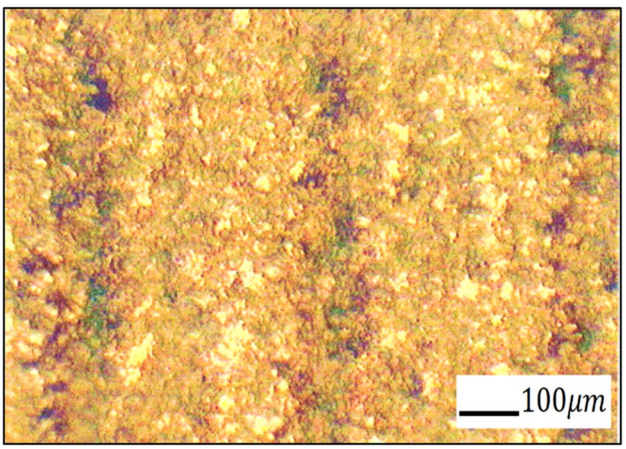

Fig. 2 Typical surface morphology of laser-nitrided Ti-6A1-4 V alloy for scanning speed, *Y* 2.5 mm/s

region of the LMZ and their density decreased in depth. The heat-affected zone (HAZ) is the second zone which is distinguished by red dashed line. Microstructure in HAZ possesses the same morphology with the substrate that represents also the non-affected zone, which is distinguished by yellow dashed line (Fig. 3).

Moreover, it appears clear from the same SEM micrograph that columnar TiN dendrites grew along a direction perpendicular to the melted surfaces; such columnar microstructures are solidified under a macroscopic temperature gradient induced by the unidirectional heat flux. In relation to our results, it has been reported in the work of Hirvonen [14] that TiN dendrites with the primary arms near perpendicular to the surface formed in top area of LMZ; additionally, $TN_{0.3}$ needles were more likely formed in area below top layer, and the titanium matrix contained fine eutectic α-Ti grains, while the cross-section morphology of nitrided samples presented by Zong [15] indicates the presence of the so-called phase transformation zone (PTZ) instead of the laser-melted zone (LMZ) and the thickness of the nitride layer is about 1.8 μm.

3.2 Microhardness and tribological behavior

Figure 4 depicts the microhardness distributions along the depth in cross-section of the samples treated under nitrogen

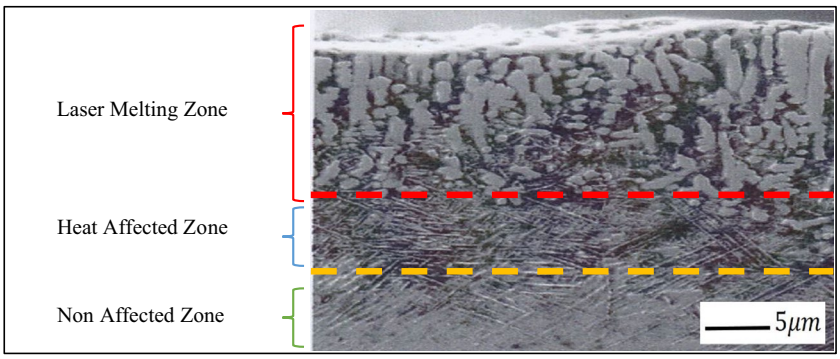

Fig. 3 SEM micrograph showing TiN dendrites growing from the continuous thin layer on the free surface of the laser-melted zone

flow of 10 l/min. The LMZ microhardness drops from 930 to 480 Hv as the distance between the surface and the depth increases. In addition, from the same figure, by analyzing the curves slope and linking them with beam scanning speeds, LMZ hardness value, and thicknesses of Laser-melted zones ranging from 2 to 8 µm, we can conclude that low scanning speed led to the thicker LMZ. Particularly, the beam scanning speed of 2.5 mm/s gives a rise to a LMZ of roughly 8 µm; in relation to our results, Dahotre [18] performed laser nitriding on Ti-6Al-4 V alloy using pure N_2 and found that TiN dendritic layers with thicknesses of 9.5, 11.3, and 13.8 µm were produced with three different laser energy densities (1.70, 1.89, and 2.12×106 J/m^2). Meanwhile, Sathish [19] found that X-ray diffraction analysis did not provide a distinct TiN signal during laser nitriding under controlled N_2 environment using a Nd-YAG pulsed laser. For the hardness increasing, it is mainly due to the solidification of cermets made of titanium nitride (TiN), acting as hard ceramic phase under the state of small dendrites which are enclosed in a metallic α-Ti matrix and are always characterized by higher hardness than that of the untreated Ti-6Al-4 V sample.

On the other hand, a comparison of the tribological characteristics of nitrided samples is illustrated in Figs. 5 and 6.

On the other hand, Fig. 5 shows the morphologies of the tracks of wear of nitrided surfaces. After 8000 turns, these tracks present different aspects: For the samples nitrided with a speed of 7.5 mm/s and 10 mm/s (Fig. 5a, b), clear aspect with some blackened zones irregularly distributed is observed, whereas for the samples irradiated with speeds of 5 mm/s and 2.5 mm/s respectively (Fig. 5c, d), a black and regular aspect with unvarying width is observed on all the circumference. Moreover, the bottom of the wear exhibits fine scratches which are oriented according to the sliding direction.

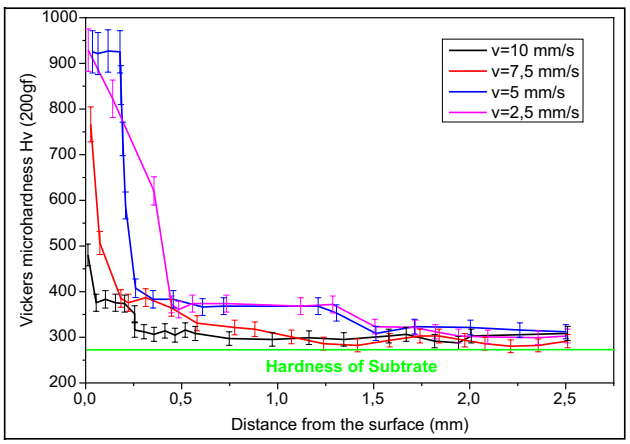

Fig. 4 Microhardness distributions along the depth in cross-section of laser-nitrided Ti-6Al-4 V alloy for different scanning speeds of laser beam

Figure 6 presents the evolutions of the friction coefficient versus sample's hardness after different numbers of turns. It is clear to notice that for the first 10 turns, the friction coefficient is about 0.2 for all the samples, and there is friction between two bodies the ball of the ruby and the fine layer of nitride of titanium; then, between 20 and 30 turns, the friction coefficient drops slightly for the sample of microhardness 450 Hv. On the other hand, it increases for the other samples and passes from 0.25 to 0.34. After 40 turns, the friction coefficient increases for all the samples reaches about 0.3 for the sample of 450 Hv and 0.4 for other samples, while from 50 turns, this coefficient continues to increase slightly to reach 0.48 in the case of the samples of the least lasts (450 Hv) and 0.47 for the sample hardest (950 Hv).Consequently, this variation of friction coefficient can be to interpreted in three stages: (i) For the first stage, there is friction between two ceramic bodies: the ball of the ruby and the layer of TiN nitride; the protuberances generated by the laser pulses buckle by plastic strain and the relief of the nitrided titanium surface is reduced. (ii) The second stage corresponds to the beginning of wear of the base of the TiN dendrites in the zone molten and nitrided by laser irradiation. (iii) In the third stage, the cyclic loading of the friction track induces plastic strains by shearing and generate microcracks by fatigue damage as shown in Fig. 7.

The nucleation and the propagation of these cracks under the nitrided titanium surface induce its fracture and wear with the formation of wear particles; these hard particles come from the breaking of titanium nitride dendrites of the molten zone, and they from an abrasive third body modifying the contact between ruby ball and nitrided titanium surface.

4 Conclusion

In this work, surface nitridation on Ti-6Al-4 V titanium alloy by means of pulsed Nd-YAG laser under nitrogen gas flow was investigated. The Ti alloy's surface was irradiated and melted at different laser scanning speeds. The following conclusions can be drawn from the different analyses performed.

- After laser melting, the solidification of laser-melted zone (LMZ) resulted in the formation of two ceramic phases: hard TiN and $TiN_{0.3}$ nitride grains inside a ductile α-Ti matrix. In addition, the TiN dendritic was observed in the upper part of the laser-melted zone
- Under optimal laser irradiation conditions (scanning speed 2.5 mm/s), the investigated titanium alloy may

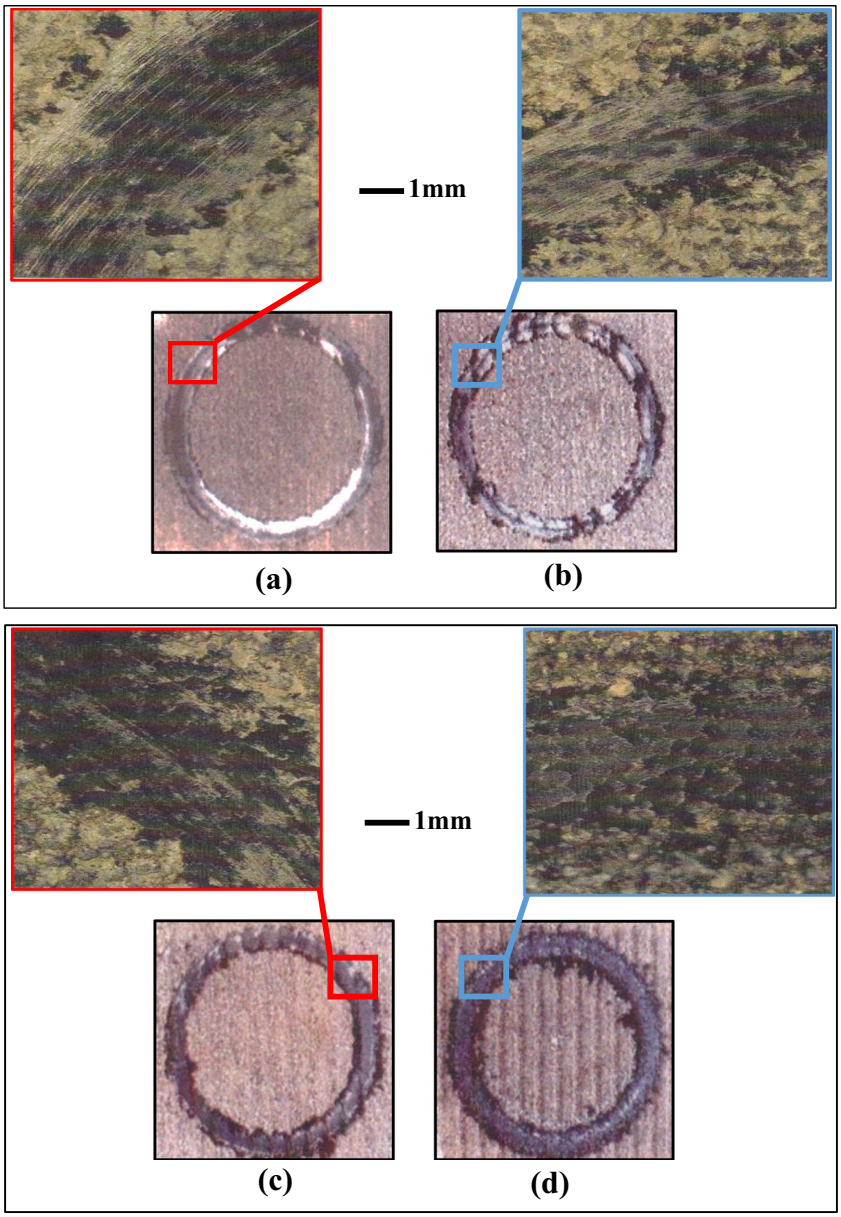

Fig. 5 Wear track of specimen after 8000 turns: **a** *V* l0 mm/s; **b** *V* 7.5 mm/s; **c** *V* 5 mm/s; **d** *V* 2.5 mm/s

achieve a surface hardness of around 950 Hv0.2, indicating high wear resistance, which is mainly attributed to the solidification of cermets made of titanium nitride (TiN) with a width of roughly 8 µm, acting as a hard ceramic phase.

- The macroscopic and microscopic examination of the friction tracks produced by using pin-on-disk tribometer revealed that the wear morphology is mainly related to the thickness of the TiN nitrided layer (2–8 µm).

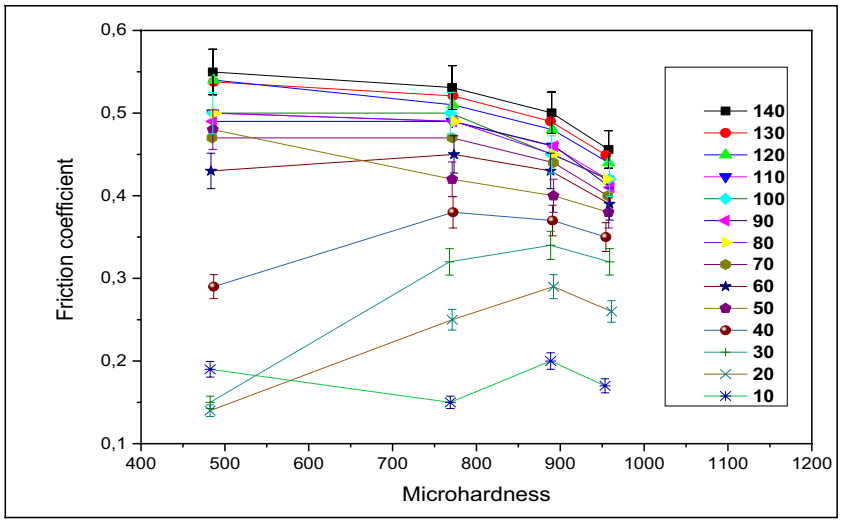

Fig. 6 Relations between friction coefficient and microhardness after different numbers of turns

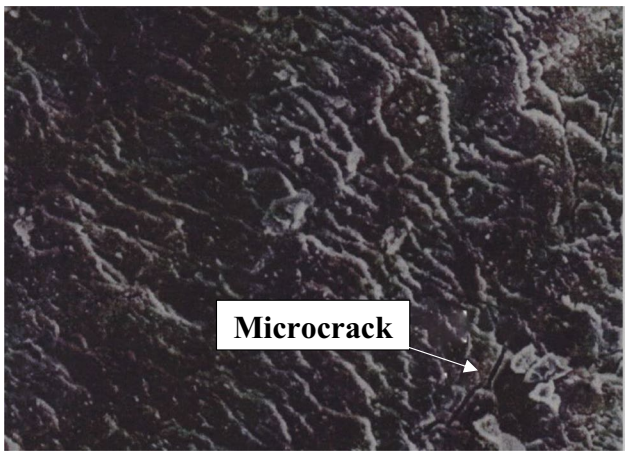

Fig. 7 SEM micrographs of the crack

Declarations

Competing interests The authors declare no competing interests.

References

1. Liu D, Ni C, Wang Y et al (2024) Zhu, Review of serrated chip characteristics and formation mechanism from conventional to additively manufactured titanium alloys. J Alloys Compd 970:172573. https://doi.org/10.1016/j.jallcom.2023.172573
2. Guo Y, Liu G, Song Y (2023) Creep behavior of titanium alloy used in deep-sea pressure shell considering tensile/compressive asymmetry: experiments and numerical modeling. Ocean Eng 288:116095. https://doi.org/10.1016/j.oceaneng.2023.116095
3. Kalyon M, Yilbas BS (2003) Laser pulse heating: a formulation of desired temperature at the surface. Opt. Lasers Eng 39(1):109–119. https://doi.org/10.1016/S0143-8166(02)00088-X
4. Zhang J, Guo H, Hu M, Xu H, Ju H,… (2003) Effect of common alloying elements on α' martensite start temperature in titanium alloys. J Mater Res Technol., 27, 4562-4572, https://doi.org/10.1016/j.jmrt.2023.10.159.
5. Fouilland-Paille L, Ettaqi S, Benayoun S, Hantzpergue JJ (1997) Structural and mechanical characterization of Ti/TiC cermet coatings synthesized by laser melting. Surf Coat Technol. 88(1):204–211. https://doi.org/10.1016/S0257-8972(96)02925-8
6. Courant B, Hantzpergue JJ, Benayoun S (1999) Surface treatment of titanium by laser irradiation to improve resistance to dry-sliding friction. Wear 236(1):39–46. https://doi.org/10.1016/S0043-1648(99)00254-9
7. Hanawa T (2022) Biocompatibility of titanium from the viewpoint of its surface. Sci Technol Adv Mater 23(1):457–472. https://doi.org/10.1080/14686996.2022.2106156
8. Sivanantham G, Pudukarai Ramaswamy T, Selvaraj S, Murugan A, Sahayaraj Arockiasamy F (2024) Adapting a phenomenological model for predicting acoustical behaviour of Camellia sinensis/Ananas comosus/E-glass fibre-blended epoxy hybrid composites. *Proc Inst Mech Eng Part J Mater Des Appl*, 14644207241237736, https://doi.org/10.1177/14644207241237736
9. Kamalakannan V, Rajaram S, Iyyadurai J, Arockiasamy FS (2024) Fundamental study on influence of independent factors on response variable using response surface methodology and Taguchi method. Eng Proc 61(1), https://doi.org/10.3390/engproc2024061037
10. Naizabekov A, Samodurova M, Bodrov E, Lezhnev S, Samoilova O, Trofimov E, Mikhailov D, Litvinyuk K, Trofimova S, Latfulina Y (2023) Use of laser cladding for the synthesis of coatings from high-entropy alloys reinforced with ceramic particles. Case Stud Constr Mater 19:e02541. https://doi.org/10.1016/j.cscm.2023.e02541
11. Saurabh A, Meghana CM, Singh PK (2022) Titanium-based materials: synthesis, properties, and applications. Mater Today Proc 56:412–419. https://doi.org/10.1016/j.matpr.2022.01.268
12. Sun B, Li S, Imai H, Mimoto T, Umeda J, Kondoh K (2013) Fabrication of high-strength Ti materials by in-process solid solution strengthening of oxygen via P/M methods. Mater Sci Eng A 563:95–100. https://doi.org/10.1016/j.msea.2012.11.058

13. Zong X, Wang H, Tang H, Cheng X, Tian X, Ran X (2023) Microstructure evolution and mass transfer behavior during multi-pass laser surface nitriding process on titanium alloy. Surf Coat Technol. 466:129565. https://doi.org/10.1016/j.surfcoat.2023.129565
14. Hirvonen JP, Koskinen J, Jervis JR, Nastasi M (1996) Present progress in the development of low friction coatings. Surf Coat Technol 80(1):139–150. https://doi.org/10.1016/0257-8972(95)02701-7
15. Zong X, Wang H, Li Z, Li J, Cheng X, Zhu Y, Tian X,.., (2020) Laser nitridation on Ti-6.5Al-3.5Mo-1.5Zr-0.3Si titanium alloy. Surf Coat Technol, 386, 125425, https://doi.org/10.1016/j.surfcoat.2020.125425.
16. Zeng C, Wen H, Ettefagh AH, Zhang B, Gao J, Haghshenas A, Raush JR,... (2020) Laser nitriding of titanium surfaces for biomedical applications. Surf Coat Technol., 385, 125397, https://doi.org/10.1016/j.surfcoat.2020.125397
17. Senthilselvan J, Monisha K, Gunaseelan M, Yamini S, Kumar SA, Kanimozhi K, Manonmani J, Shariff SM, Padmanabham G,… (2020) High power diode laser nitriding of titanium in nitrogen gas filled simple acrylic box container: microstructure, phase formation, hardness, dendrite and martensite solidification analyses. Mater Charact., 160, 110118, https://doi.org/10.1016/j.matchar.2020.110118
18. Dahotre SN, Vora HD, Rajamure RS, Huang L, Banerjee R, He W,… (2014) Laser induced nitrogen enhanced titanium surfaces for improved Osseo-integration. *Ann Biomed Eng.*, 42(1): 50-61, https://doi.org/10.1007/s10439-013-0898-z
19. Sathish S, Geetha M, Pandey ND, Richard C, Asokamani R (2010) Studies on the corrosion and wear behavior of the laser nitrided biomedical titanium and its alloys. Mater Sci Eng C 30(3):376–382. https://doi.org/10.1016/j.msec.2009.12.004